Microwave Band Demonstration of a Reflective Geometry Fiber and Free-Space Binary Photonic Delay Line

Nabeel A. Riza and Nicholas Madamopoulos

***Abstract*— For the first time, a modulated 2-b, one-channel binary switched, photonic time delay system (PTDS) is demonstrated that is based on a compact reflective optical delay path geometry that consists of one free-space delay line and one non-polarization-maintaining (PM) fiber delay line. Polarization switching using birefringent-mode nematic liquid crystals and a polarization noise-reduction technique are used to minimize the optical noise when using the cube polarization beamsplitters (PBS's) required in the reflective geometry delay. This gives the high electrical signal-to-noise ratios measured from 52 to 89 dB for the four settings of the delay line.**

***Index Terms*— Liquid crystal, optical fiber, phased-array antennas, photonic delay lines.**

I. Introduction

OPTOELECTRONICS has been proposed for making photonically controlled phased array systems [1]–[5]. In particular, at high electrical signal frequencies, such as the microwave and millimeter-wave bands, photonic processing can offer significant advantages such as large instantaneous and tunable signal processing bandwidths, along with compact and lightweight processing modules and protection from electromagnetic interference (EMI). Over the past few years, we have proposed a variety of optically incoherent (intensity modulation-based), multichannel, free-space, solid-optics, and fiber-based photonic time delay architectures for reversible transmit–receive mode phased array antennas [6]. These architectures are based on two-dimensional (2-D) pixelated optical arrays based on polarization optical switching. We have successfully demonstrated high on/off optical isolation ($>$35 dB) light beam switching using birefringent-mode nematic liquid crystals (NLC's) [7]. These NLC switches also demonstrated moderately fast optical switching (e.g., 1 ms) using the transient nematic effect employing high voltage (e.g., 10 V_{peak}) switch drive electronics. These moderately fast NLC optical switches form the basis of our proposed photonic time delay architectures using spatial light modulators (SLM's) where moderately fast ($<$1000 beams/s) antenna beam switching is adequate for the antenna application using a time-multiplexed antenna scanning node [8]. We have recently conducted a 25-channel NLC-based time delay unit characterization experiment demonstrating low channel-to-channel electrical crosstalk (e.g., $-$42 dB) values when imaging optics is used in the unit [9].

An important issue with our three-dimensional (3-D) photonic time delay architectures is mechanical stability and size, particularly in cases where long time delays ($>$5 ns) are required for the most significant bit (MSB) in the binary delay line architecture. Recently, we have proposed [10] and demonstrated [11] a novel reflective geometry photonic delay line design that uses a shorter/compacter optical delay path for time delay implementation. Using this reflective design with a special polarization noise reduction scheme and a fiber-birefringence compensation method, it becomes possible to use free-space, solid-optics, and non-polarization-maintaining fiber-based optical delay paths that are smaller, lighter, and more compressed (in volume) than previous transmissive designs. As such, we can expect greater mechanical stability from our new reflective designs that use the cube PBS's.

In this letter, we demonstrate for the first time a 2-b structure of the compact reflective geometry delay line, using a 1-GHz microwave band optical modulation of the input laser beam. Microwave frequency optical modulation via an acoustooptic modulator (AOM) system is introduced for characterization of the photonic time delay system (PTDS) in the radio frequency (RF) domain using RF spectrum analyzer measurements, and these results are described in this letter [12].

II. Experimental 2-B PTDS at 1 GHz

The experimental setup for the 2-b one-channel PTDS is depicted in Fig. 1. A 632.8-nm 10-mW CW He–Ne laser is used as an input to the dual AOM-based optical modulation system, as described in earlier work [8]. To obtain the 1-GHz optical modulation that is transmitted through the PTDS, the two AOM's are fed by a 500-MHz signal, resulting in two collinear beams with a relative Doppler shift of 1 GHz. Hence, 1-GHz (frequency modulated) CW light beam enters the PTDS.

The PTDS works as follows. Vertical or s-polarized light passes through the first polarizer (vertical polarizer). SLM1 acts as a switch to either change the polarization to horizontal or p-polarization when it is set in its "on" state, or leaves the input polarization unchanged if it is set in the "off" state.

Manuscript received October 31, 1996. This work was supported by the Office of Naval Research, Program Monitor Dr. W. Miceli, under Grant N000149510988.

The authors are with the Center for Research and Education in Optics and Lasers (CREOL) and the Department of Electrical and Computer Engineering, University of Central Florida, Orlando, FL 32816-2700 USA.

Publisher Item Identifier S 1051-8207(97)02509-9.

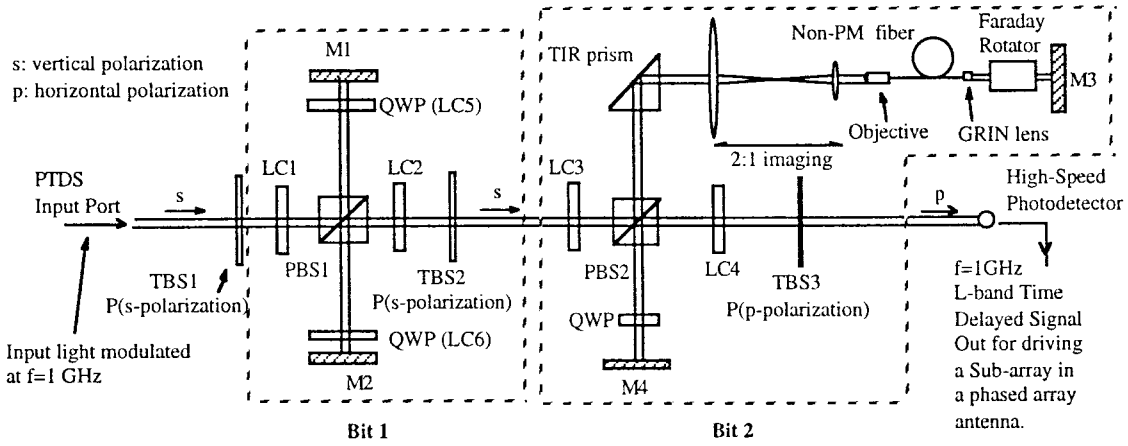

Fig. 1. The experimentally demonstrated 2-b, one-channel switched photonic delay line setup using the compact reflective geometry in the delay paths. The experiment is performed at a 1-GHz optical modulation frequency using a 633-nm visible input light beam.

The cube PBS (PBS1) acts as a path selector, directing light depending on the polarization of the incident beam. When p-polarized light hits the PBS 1, it travels straight through toward the SLM2. SLM2 is set in the "on" state and thus changes the incident p-polarization to s-polarization, which then passes through the second vertical polarizer toward the second bit of the PTDS. On the other hand, when SLM1 is set in its "off" state, the light stays s-polarized and is deflected from PBS1 toward the quarter-wave plate (QWP), which has its axis at 45° with respect to the incident s-polarization. The s-polarized light hits the QWP, and after reflection from the mirror, the beam is redirected through the QWP and becomes p-polarized. Then, this light passes through PBS1 and hits another QWP that has its axis at 45° with the incident p-polarization. After reflection from the mirror (M2), passes through the QWP and becomes s-polarized. This s-polarized light is deflected by an angle of 90° from the PBS 1 toward the SLM2. This SLM is set in the "off" state, which does not change the incident polarization. s-polarization passes through the vertical polarizer (P2) toward the second bit of the PTDS. The same procedure can be applied for the second bit. The difference in this bit is that the delay path consists of a fiber delay, and thus, instead of a QWP, a Faraday rotator is used, as this can compensate for any induced birefringence of the fiber [11].

The components used in the experiment include parallel-rub birefringent mode NLC devices LC1, LC2, LC3, LC4, LC5, and LC6, which are inserted with their NLC directors at 45° with the incident s or p linear polarization. LC1, LC2, LC3, and LC4 act as high-performance polarization rotators. LC5 and LC6 act as QWP's. Two broad-band cube PBS's are used with a specified extinction ratio (p/s) for the straight port of $>1000:1$. The extinction ratio (s/p) for the reflected port was measured as $<50:1$. Thompson beamsplitting (TBS's) polarizers with a high extinction ratio of $>10\,000:1$ are also used at both ports. 40 and 20 cm focal length (FL) biconvex spherical lenses are used for $2:1$ imaging of the beam for better coupling efficiency into the cleaved fiber face. In addition, the objective lens is a $\times 40$, NA $= 0.65$, FL $= 4.3$ mm device and the fiber is a non-PM single mode fiber at 632.8 nm. A GRIN collimator-lens is attached to one end of the fiber and the other end is cleaved.

TABLE I
MEASURED TRANSMISSION/REFLECTION EFFICIENCIES OF THE OPTICAL COMPONENTS

Optical component	Efficiencies (%)	Optical component	Efficiencies (%)	Optical component	Efficiencies (%)
LC1	82.55	PBS1 straight	88.7	QWP	96.0
		reflected	97.0		
LC2	88.89	PBS2 straight	82.0	Fiber	1st bit straight
		reflected	89.0	coupling	25.0
LC3	88.80	TBS	90.0	system	1st bit delay
					22.0
LC4	91.10	TIR prism	92.97	Faraday	
LC5	89.97	Lenses	L1 90.8	Rotator	96.0
LC6	88.00		L2 92.2	Mirror	97.0

TABLE II
EXPECTED AND MEASURED OPTICAL LOSS FOR THE FOUR SETTINGS OF THE PTDS

PTDS Settings	Expected Optical Loss* (dB)	Measured Optical Loss** (dB)
1st Bit - straight 2nd Bit -straight	-4.56	-4.95
1st Bit - delay 2nd Bit -straight	-7.08	-10.50
1st Bit -straight 2nd Bit - delay	-20.77	-20.15
1st Bit - delay 2nd Bit - delay	-24.43	-20.85

*Expected loss data were calculated using measured optical component efficiencies.
**Experimental data were calculated using rf spectrum analyzer measurements.

Based on the measured transmission/reflection efficiencies of the optical components (Table I), the expected and measured optical losses for the four settings of the PTDS are shown in Table II. For the delay paths, a higher loss is anticipated due to the greater number of nonantireflection (AR)-coated optical components used in this path. In addition, the second bit delay path fiber-coupling assembly has a low near 25% optical transmission, which plays a significant role (>12-dB RF loss) in the overall loss budget. The L-band signal modulation is photo-detected using a high-speed New Focus

TABLE III
RF SNR FOR THE FOUR SETTINGS OF THE PTDS WITH AND WITHOUT THE NOISE-REDUCTION SCHEME. (A: MEASURED AT THE OUTPUT OF THE FIRST BIT; B: MEASURED AT THE OUTPUT OF THE SECOND BIT)

PTDS Output Measurement Setting	Electrical SNR at 1GHz (dB) without noise reduction	Electrical SNR at 1GHz (dB) with noise reduction
1st Bit - straight, A	49.3	89.8
1st Bit - delay, A	24.8	75.4
2nd Bit -straight (1st Bit - straight), B	82.0	83.0
2nd Bit -straight (1st Bit - delay), B	64.0	62.5
2nd Bit - delay (1st Bit -straight), B	23.68	48.40
2nd Bit - delay (1st Bit - delay), B	49.4	52.33

Model 1601 photoreceiver. Spectrum analyzer measurements are used to determine electrical loss values of -9.9, -21.0, -40.3, and -41.7 dB for the first, second, third, and fourth setting, respectively. Since the spectrum analyzer gives direct electrical power measurements, we have to divide the above measurements by two to get the optical power values that, except for the fourth case, are very close to the expected optical losses. All expected loss values are calculated assuming that all the input light energy travels through the selected optical paths in the delay line. In the experimental scenario, the finite on/off optical switching ratios for the SLM's causes some input light to travel through the unselected paths. For the four different delay line settings, this unwanted leakage light, which adds to the final output desired light energy, can have different energy levels. In our fourth setting, this leakage light is relatively high enough compared to the desired path light, indicating a higher observed optical power than expected. Hence, the 3.6-dB difference.

Signal-to-noise ratio (SNR) measurements were obtained for all four settings of the PTDS. We define SNR as $10\log$(*signal* power/*noise* power). As *signal*, we define the optical power in the optical beam of the desired polarization that travels through the desired delay or straight path of the bits; all other optical power measured at the output is regarded as *noise* optical power. The key optical/rf noise introduced by our PTDS to the L-band signal was the optical switch leakage noise and the highest leakage noise was measured as -117 dBm, when the first bit was set for delay and the second bit was set for the straight path.

Table III shows that the noise reduction scheme is "vital" for generating high SNR's from the PTDS. Moreover, the cascading architecture of our noise-reduction scheme reduces the noise transmitted from bit to bit in the N-bit delay line structure. Hence, noise originating from the first bit time delay structure is rejected by the noise reduction scheme and will not be transmitted toward the next time delay bit. In our experimental case, for the no-delay case of the second bit, the SNR improvement is not as high because the noise level is very low due to the high noise energy attenuation in the fiber delay path.

Spectrum analyzer measurements showed that the optical system does not introduce any additional electromagnetic pick-up from the surrounding test environment, as the RF spectrum floor over the entire RF spectrum analyzer bandwidth (outside the center frequency) remains the same no matter which of the four PTDS settings is selected. This floor was measured to be lower than -128 dBm. The major effect of the optical system is the attenuation of the l-GHz L-band optically modulated carrier signal, and this limitation can be overcome by the use of AR-coated optical components and, in particular, higher efficiency fiber-coupling.

III. CONCLUSION

In conclusion, we have demonstrated at L-band, for the first time, a 2-b, one-channel, NLC-based PTDS using the novel compact reflective geometry for one free-space and one non-PM fiber delay path. Worst case RF SNR's of around 50 dB were obtained. High losses were present in our test system due to the non-AR-coated optical components with a typical 90% efficiency, and more importantly, via the low 25% transmission of the objective-to-fiber coupling system. These losses can be minimized by the use of AR-coated optical components and better fiber-coupling optics, giving higher signal power and thus higher SNR. Our noise reduction scheme plays a critical role in suppressing noncoherent (or orthogonal polarization) noise in the PTDS, resulting in higher RF SNR's. Future work relates to building a lower loss single-bit PTDS for realizing N-bit M-channel systems and work to study coherent (or same polarization) noise effects.

REFERENCES

[1] R. A. Soref, "Voltage controlled optical/RF phase shifter," *J. Lightwave Technol.*, vol. LT-3, pp. 992–998, 1985.
[2] I. Frigyes and A. J. Seeds, "Optically generated true-time delay in phased array antennas," *IEEE Trans. Microwave Theory Tech.*, vol. 43, Sept. 1995.
[3] D. Dolfi, P. Joffre, J. Antoine, J.-P. Huignard, D. Philippe, and P. Granger, "Experimental demonstration of a phased array antenna optically controlled with phase and time delays," *Appl. Opt.*, vol. 35, no. 26, pp. 5293–5300, Sept. 10, 1996.
[4] A. Daryoush, P. Herczfeld, V. Contario, A. Rosen, Z. Turski, and P. Wahi, "Optical beam control of mm-wave phased array for communications," *Microwave J.*, vol. 30, no. 3, pp. 97–104, Mar. 1987.
[5] K. Horikawa, Y. Nagasuga, and H. Ogawa, "Self-heterodyning optical waveguide beamforming and beam steering network integrated on lithium niobate substrate," *IEEE Trans. Microwave Theory Tech.*, vol. 43, pp. 2395–2401, Sept. 1995.
[6] N. A. Riza, "Liquid crystal-based optical time delay units for phased array antennas," *J. Lightwave Technol.*, vol. 12, pp. 1440–1447, Aug. 1994.
[7] ——, "High optical isolation low loss moderate switching speed nematic liquid crystal optical switch," *Opt. Lett.*, vol. 19, no. 8, pp. 1780–1782, 1994.
[8] ——, "Liquid crystal-based optical control of phased array antennas," *J. Lightwave Technol.*, vol. 10, pp. 1974–1984, Dec. 1992.
[9] ——, "25-channel nematic liquid crystal optical time-delay unit characterization," *IEEE Photon. Technol. Lett.*, vol. 7, pp. 1285–1287, Nov. 1995.
[10] ——, "Polarization-based fiber optic delay lines," in *SPIE Proc.*, 1995, vol. 2560, pp. 120–129.
[11] N. A. Riza and N. Madamopoulos, "High signal-to-noise ratio birefringence compensated optical delay line based on a noise reduction scheme," *Opt. Lett.*, vol. 20, no. 22, pp. 2351–2353, 1995.
[12] N. Madamopoulos, "Photonics for antenna applications," *Optics and Photonics News, OSA Mag.*, vol. 7, no. 11, Nov. 1996.